



Title	Magnetic torque and ac and dc magnetic susceptibility measurements on $\text{PTMA}_{0.5}[\text{Fe}(\text{Pc})(\text{CN})_2] \cdot \text{CH}_3\text{CN}$: Origin of spontaneous magnetization in $[\text{Fe}(\text{Pc})(\text{CN})_2]$ molecular conductors
Author(s)	Tajima, Hiroyuki; Yoshida, Gosuke; Matsuda, Masaki; Yamaura, Jun-Ichi; Hanasaki, Noriaki; Naito, Toshio; Inabe, Tamotsu
Citation	Physical Review B, 80(2), 024424 https://doi.org/10.1103/PhysRevB.80.024424
Issue Date	2009-07
Doc URL	http://hdl.handle.net/2115/39046
Rights	©2009 The American Physical Society
Type	article
File Information	PRB80-2_024424.pdf



[Instructions for use](#)

Magnetic torque and ac and dc magnetic susceptibility measurements on $\text{PTMA}_{0.5}[\text{Fe}(\text{Pc})(\text{CN})_2] \cdot \text{CH}_3\text{CN}$: Origin of spontaneous magnetization in $[\text{Fe}(\text{Pc})(\text{CN})_2]$ molecular conductors

Hiroyuki Tajima, Gosuke Yoshida, Masaki Matsuda, and Jun-Ichi Yamaura
Institute for Solid State Physics, The University of Tokyo, Kashiwa, Chiba 277-8581, Japan

Noriaki Hanasaki

Department of Physics, Faculty of Science, Okayama University, Okayama, Okayama 700-8530, Japan

Toshio Naito and Tamotsu Inabe

Division of Chemistry, Graduate School of Science, Hokkaido University Kita-ku, Sapporo 060-0810, Japan

(Received 25 November 2008; revised manuscript received 28 April 2009; published 24 July 2009)

Magnetic torque ($3 \leq T \leq 46$ K), dc magnetic susceptibility ($2 \leq T \leq 300$ K), and ac magnetic susceptibility ($2 \leq T \leq 30$ K) are reported for $\text{PTMA}_{0.5}[\text{Fe}(\text{Pc})(\text{CN})_2] \cdot \text{CH}_3\text{CN}$. The torque curves exhibit a sinusoidal line shape for temperatures above 6 K. This result as well as the temperature dependence of the dc magnetic susceptibility above 13 K was analyzed by employing an anisotropic Heisenberg model in one dimension. The compound exhibits spontaneous magnetization below 6 K. The torque measurements at 3 K revealed that the direction of this spontaneous magnetization is parallel to the easy axis of the mother antiferromagnetism. The ac susceptibility measurements demonstrated the fluctuation of the spontaneous magnetization up to 13 K. A model of charge-ordered ferrimagnetism is proposed in order to explain these results. This model explains the spontaneous magnetization which commonly appears in conducting salts of $[\text{Fe}(\text{Pc})(\text{CN})_2]$ and their derivatives.

DOI: [10.1103/PhysRevB.80.024424](https://doi.org/10.1103/PhysRevB.80.024424)

PACS number(s): 75.47.De, 75.30.Gw, 75.50.Xx

I. INTRODUCTION

The $[\text{Fe}(\text{Pc})(\text{CN})_2]$ molecule (Fig. 1; Pc=phthalocyanine) has a unique feature from the viewpoints of spintronics and magnetism. The d electrons of Fe(III) at the center of the Pc ring are in a low-spin state with $S=1/2$. Because of the four-fold symmetry of $[\text{Fe}(\text{Pc})(\text{CN})_2]$, the orbital magnetic moment of Fe(III) is not completely quenched. Consequently, the d electrons in Fe(III) behave as a local magnetic moment with highly anisotropic g factors. ($g_{xx}=0.52$, $g_{yy}=1.11$, and $g_{zz}=3.62$ in the case of PNP $[\text{Fe}(\text{Pc})(\text{CN})_2]$.¹ See the definition of the xyz principal axes in the g tensor shown in Fig. 1.) On the other hand, the π electrons originating from the Pc ring of $[\text{Fe}(\text{Pc})(\text{CN})_2]$ are a potential source of conduction electrons. Since the d and π electrons belong to the same molecule, a large d - π interaction is inherently expected in $[\text{Fe}(\text{Pc})(\text{CN})_2]$.

Up to now, there have been several molecular conductors reported for the charge-transfer salts of $[\text{Fe}(\text{Pc})(\text{CN})_2]$ and their derivatives, TPP $[\text{Fe}(\text{Pc})\text{Br}_2]_2$ and TPP $[\text{Fe}(\text{Pc})\text{Cl}_2]_2$.²⁻⁶ All the reported salts have three-quarter-filled one-dimensional bands and exhibit giant negative magnetoresistance (GNMR). This GNMR is an interesting phenomenon both experimentally and theoretically.⁷ In the case of TPP $[\text{Fe}(\text{Pc})(\text{CN})_2]_2$, the resistance ratio $R(H)/R(0)$ is less than 0.01 at $T=20$ K and $H=350$ kOe.⁸ It is not caused by a phase transition such as the field-induced metal-insulator transition observed in the manganese oxides⁹ and λ -(BETS) $_2\text{FeCl}_4$.¹⁰ It is highly anisotropic in regard to the magnetic-field direction reflecting the molecular orientations of $[\text{Fe}(\text{Pc})(\text{CN})_2]$. This tendency is qualitatively explained by considering the large g -factor anisotropy of Fe(III).¹¹

In order to study this GNMR phenomenon in detail, the magnetic states of both d - and π -electron systems should be clarified on the basis of microscopic pictures. Recently we have measured the magnetic torque and heat capacity of TPP $[\text{Fe}(\text{Pc})(\text{CN})_2]_2$ salt and analyzed them together with magnetic susceptibility data on the basis of the one-dimensional anisotropic Heisenberg model.¹² Our study revealed that: (i) the peak in the magnetic susceptibility data around 25 K is due to the antiferromagnetic short-range order of d electrons; (ii) π electrons fall into an antiferromagnetic state below 13 K, with fluctuations of state appearing even at 17 K; and (iii) an anomalously large spin-flop field (80 kOe at 9 K) is observed for the π -electron antiferromagnetic state. We also proposed that: (iv) magnetic behaviors of conducting $[\text{Fe}(\text{Pc})(\text{CN})_2]$ salts are essentially governed by exchange interactions within the $[\text{Fe}(\text{Pc})(\text{CN})_2]$ chain; (v) the π electrons below 13 K are not in a genuine antiferromagnetic state, and accompanied by a parasitic ferromagnetism; (vi) this parasitic ferromagnetism may cause the GNMR. On the other hand, the origin of this parasitic ferro-

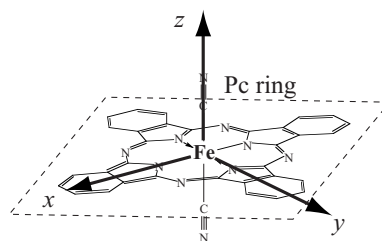


FIG. 1. Molecular structure of $[\text{Fe}(\text{Pc})(\text{CN})_2]$ and the definition of xyz principal axes in the g tensor of Fe(III) in $[\text{Fe}(\text{Pc})(\text{CN})_2]$.

magnetism was not clarified in the previous report. Here in this paper we present a possible mechanism of this unique magnetism widely found in the conducting $[\text{Fe}(\text{Pc})(\text{CN})_2]$ salts.

In the studies of parasitic ferromagnetism, it is quite important to determine the direction of spontaneous magnetization in relation to the easy axis of the antiferromagnetism, which is the mother of the parasitic ferromagnetism. For example, the direction of the spontaneous magnetization is perpendicular to the easy axis in the case of canted antiferromagnetism, which is a possible origin of the parasitic ferromagnetism. On the other hand, the direction is parallel to the easy axis in the case of the ferrimagnetism, which is another possible origin.

The $[\text{Fe}(\text{Pc})(\text{CN})_2]$ salts are a complicated system composed of d and π electrons. Both can form an antiferromagnetic order. However, we can infer that the easy axis of the antiferromagnetic order should be parallel to the CN axis of $[\text{Fe}(\text{Pc})(\text{CN})_2]$ in either case. The reason is that this direction coincides with that of the largest g factor of the Fe(III) d electrons in $[\text{Fe}(\text{Pc})(\text{CN})_2]$ and the magnetic anisotropy energy of π electrons arises from the d - π interaction. In fact, we have successfully reproduced the magnetic torque curve of $\text{TPP}[\text{Fe}(\text{Pc})(\text{CN})_2]_2$ within the ab plane below 13 K on the basis of the assumption that the easy axis of the antiferromagnetic π electrons is parallel to the CN axis of $[\text{Fe}(\text{Pc})(\text{CN})_2]$.¹²

By taking this into account, we can clarify the origin of the parasitic ferromagnetism if we could determine the direction of the spontaneous magnetization. However, $\text{TPP}[\text{Fe}(\text{Pc})(\text{CN})_2]_2$ salt, which we have previously studied, has four equivalent $[\text{Fe}(\text{Pc})(\text{CN})_2]$ molecules connected by a fourfold screw axis in the unit cell. This made it impossible to determine the direction of the spontaneous magnetization in relation to the easy axis, which should be parallel to the CN axis of the $[\text{Fe}(\text{Pc})(\text{CN})_2]$ molecule. Thus, we have chosen $\text{PTMA}_{0.5}[\text{Fe}(\text{Pc})(\text{CN})_2] \cdot \text{CH}_3\text{CN}$ [PTMA: phenyltrimethylammonium= $(\text{C}_6\text{H}_5)(\text{CH}_3)_3\text{N}$] in this magnetic torque measurement.³

Figure 2 shows the crystal structure of $\text{PTMA}_{0.5}[\text{Fe}(\text{Pc})(\text{CN})_2] \cdot \text{CH}_3\text{CN}$ ($Pnmm$: $a = 13.900$ Å, $b = 7.332$ Å, $c = 16.317$ Å, and $Z = 1$) (Ref. 3) and the angle θ , which defines the magnetic field direction. The starting point of θ is parallel to the a axis. The $[\text{Fe}(\text{Pc})(\text{CN})_2]$ molecules form a one-dimensional chain along the b axis. The point of this structure is that the projection of the CN axis in $[\text{Fe}(\text{Pc})(\text{CN})_2]$ onto the ac plane is parallel to the a axis. Then, we can determine the direction of spontaneous magnetization from the torque measurements for the field rotated within the ac plane, and clarify the relation between the easy axis and the spontaneous magnetization.

In this paper, on the basis of the magnetic torque and dc magnetic susceptibility measurements above 6 K, below which spontaneous magnetization occurs, we first show that the magnetic properties of this salt above ~ 20 K are well explained by the one-dimensional Heisenberg model, and propose the fluctuation of the parasitic ferromagnetism below ~ 20 K. Then, we determine the direction of the spontaneous magnetization of $\text{PTMA}_{0.5}[\text{Fe}(\text{Pc})(\text{CN})_2] \cdot \text{CH}_3\text{CN}$ based on the torque measurements at 3 K. We also report the

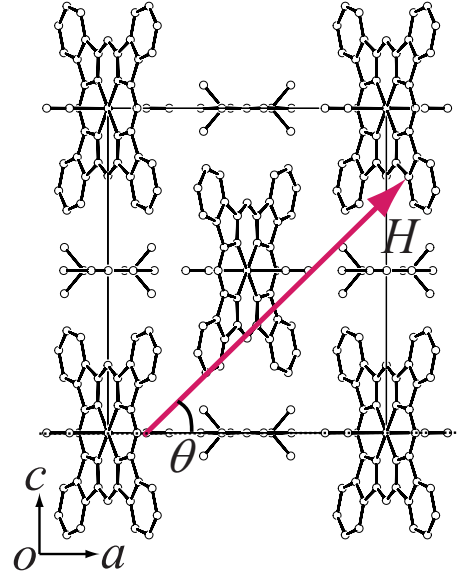


FIG. 2. (Color online) The crystal structure of $\text{PTMA}_{0.5}[\text{Fe}(\text{Pc})(\text{CN})_2] \cdot \text{CH}_3\text{CN}$ within the ac plane and the definition of the angle θ in the magnetic torque measurements.

ac susceptibility data indicating that the increase in the dc susceptibility below 13 K is a symptom of spontaneous magnetization below 6 K. By taking into account all the experimental results, we discuss the origin of the parasitic ferromagnetism which is commonly observed in $[\text{Fe}(\text{Pc})(\text{CN})_2]$ salts.

II. EXPERIMENTAL

The dc and ac magnetic susceptibilities are, respectively, measured using Magnetic Property Measurement System (MPMS) and Physical Property Measurement System (PPMS) manufactured by Quantum Design Co. Magnetic torque was measured using commercially available contact-type cantilevers of two kinds (NPX1CTP003 and SSI-SS-ML-PRC400, Seiko Instruments). The former is a standard-type cantilever used for Atomic Force Microscopy (AFM) (Nanopics, Seiko Instruments). A molding of black resin covers electrical wires in this cantilever. The latter is a cantilever specialized for low-temperature experiments. In this cantilever, electrical wires are uncovered.

We developed the experimental technique originally reported by Ohmich and Osada.¹³ Figure 3(a) shows the bridge circuit used for our measurements. The two resistors, R_r and R_s denote the piezoresistive paths for a reference and a sample, respectively. The values of R_r and R_s are almost the same, 700~600 ohms at room temperature, and 550~450 ohms at 10 K. Film resistors of equal resistance are used for R_1 and R_2 in the bridge circuit. Their typical resistance was 100 kohms. The entire bridge circuit was incorporated in the cryostat. We applied an appropriate bias voltage between A and B and measured V_{CD} and V_{EF} . This procedure enables one to cancel the resistances of the lead wires. Since the absolute values of R_s and R_r are influenced by temperature, magnetic-field strength, and magnetic-field orientation,

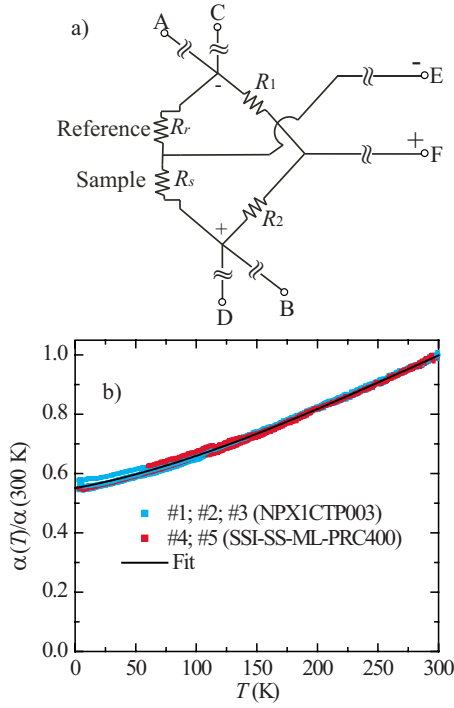


FIG. 3. (Color online) (a) A bridge circuit used for cantilever magnetometry. The circuit is incorporated in the cryostat. The six terminals (A~F) are outside the cryostat. (b) Temperature dependence of the normalized inverse sensitivity, $\alpha(T)/\alpha(300\text{ K})$ as a function of temperature. The temperature dependence of the inverse sensitivity is approximated by $\alpha(T)/\alpha(300\text{ K})=a_0+a_1T+a_2T^2+a_3T^3$, $a_0=0.551$, $a_1=7.51 \times 10^{-4}\text{ (K}^{-1}\text{)}$, $a_2=3.82 \times 10^{-6}\text{ (K}^{-2}\text{)}$, and $a_3=-4.50 \times 10^{-9}\text{ (K}^{-3}\text{)}$. As for the definition of $\alpha(T)$, see Eq. (1).

we evaluated $V_{\text{EF}}/V_{\text{CD}}$ as the final output from the bridge circuit. Ideally, this output should be a relative change in R_s against R_r+R_s , and proportional to the torque applied to the cantilever. Actually, the output contains a small offset arising from the nonequivalency in R_s/R_r or in R_1/R_2 .

On the basis of experiments using graphite as a standard sample, we found the bridge output, $\Delta V_{\text{EF}}/V_{\text{CD}}$, to be in proportional to the torque as far as the output is within $\pm 0.4\%$. In this region, magnetic torque is given by

$$\tau(T) = \alpha(T) \times (\Delta V_{\text{EF}}/V_{\text{CD}}), \quad (1)$$

where T is the temperature and $\alpha(T)$ is inverse sensitivity, which is an appropriate function of the temperature. Outside of the region, $\Delta V_{\text{EF}}/V_{\text{CD}}$ is no more linearly proportional to the torque, although qualitative measurements are possible.

Figure 3(b) shows the plot of $\alpha(T)/\alpha(300\text{ K})$ as a function of T . The α values are determined for three cantilevers of NPX1CTP003 (#1-#3) and two cantilevers of SSI-SS-ML-PRC400 (#4, #5). Five graphite samples with different weight ($68\ \mu\text{g} \pm 2\ \mu\text{g}$; $45\ \mu\text{g} \pm 2\ \mu\text{g}$; $38\ \mu\text{g} \pm 2\ \mu\text{g}$; $24.5\ \mu\text{g} \pm 2\ \mu\text{g}$; $48\ \mu\text{g} \pm 2\ \mu\text{g}$) were, respectively, attached to the cantilevers (#1-#5) by using epoxy resin (Araldite). As can be seen from the figure, curves of this function are almost the same for all the cantilevers, and are approximated by

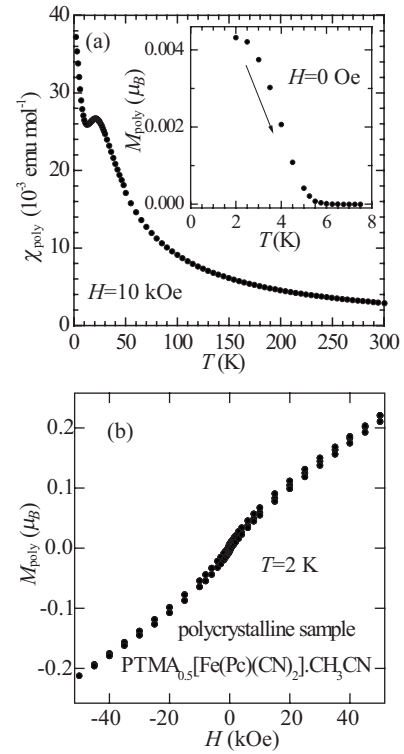


FIG. 4. (a) Temperature dependence of the magnetic susceptibility for bulk polycrystalline samples of $\text{PTMA}_{0.5}[\text{Fe}(\text{Pc})(\text{CN})_2] \cdot \text{CH}_3\text{CN}$. The inset shows the spontaneous magnetization measured at the zero field. (b) Magnetization at 2 K, as a function of the field for a polycrystalline sample. Note the anomaly around $H=0$.

$$\alpha(T)/\alpha(300\text{ K}) = a_0 + a_1T + a_2T^2 + a_3T^3, \quad (2)$$

where the coefficients are $a_0=0.551$, $a_1=7.51 \times 10^{-4}\text{ (K}^{-1}\text{)}$, $a_2=3.82 \times 10^{-6}\text{ (K}^{-2}\text{)}$, and $a_3=-4.50 \times 10^{-9}\text{ (K}^{-3}\text{)}$, respectively. We also found the α values at 300 K are consistent with an error of 5% as long as we use the cantilever chips manufactured in the same batch. This means that once we choose a chip in one batch and calibrate it, we can evaluate the absolute sensitivity of the other chips in the same batch. We determined the absolute values of the magnetic torque in this way.

Here, we would like to briefly define the sign of the torque. This is quite important in the analysis of the torque curves. In this paper, we define the sign such that a sample is dynamically in the most stable state when $\tau=0$ and $d\tau/d\theta > 0$. The crystal axes are determined using the x-ray diffraction technique.

III. RESULTS

Figure 4(a) shows the temperature dependence of the dc magnetic susceptibility for bulk polycrystalline samples of $\text{PTMA}_{0.5}[\text{Fe}(\text{Pc})(\text{CN})_2] \cdot \text{CH}_3\text{CN}$ measured under a field of 10 kOe.¹⁴ The inset of the figure shows the temperature dependence of the spontaneous magnetization measured at the zero field for samples cooled in a 50 kOe field from 30 to 2 K. The inset clearly shows that the spontaneous magnetiza-

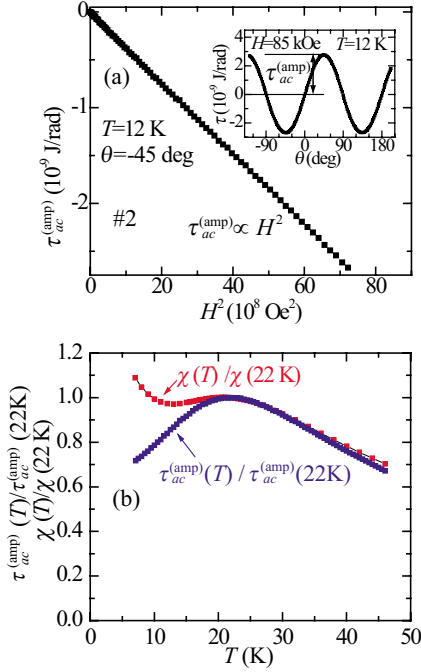


FIG. 5. (Color online) (a) Magnetic torque amplitude at 12 K for the field rotated within the crystallographic ac plane [$\tau_{ac}^{(amp)}$] plotted as a function of H^2 . The inset shows the torque curve at 12 K and $H=85$ kOe. (b) Normalized dc magnetic susceptibility and torque amplitude as a function of a temperature. Note the discrepancy below ~ 20 K.

tion disappears above ~ 6 K. Figure 4(b) shows the dc magnetization as a function of the magnetic field. The anomaly due to the spontaneous magnetization appears in the field range below $|H| < 10$ kOe. In higher field range, the magnetization curve is almost proportional to the field. As can be seen from the absolute value of the magnetization, the spontaneous magnetization of this compound is not due to a genuine ferromagnetism but due to a parasitic ferromagnetism. It should be noted that similar data of magnetic susceptibility and magnetization are reported for TPP[Fe(Pc)(CN) $_2$] $_2$ (Refs. 12 and 15) and PXX[Fe(Pc)(CN) $_2$].⁵

Figure 5(a) shows the magnetic torque amplitude at 12 K for the field rotated within the crystallographic ac plane [$\tau_{ac}^{(amp)}$] plotted as a function of H^2 . The inset shows the torque curve at the same temperature. These figures indicate that the magnetic torque is almost proportional to $H^2 \sin 2\theta$. Figure 5(b) shows the temperature dependence of the torque amplitude compared with that of the dc magnetic susceptibility shown in Fig. 4(a). As can be seen from the figure, the two curves are consistent above 20 K, below which a discrepancy becomes apparent. A similar discrepancy was found in our previous studies on TPP[Fe(Pc)(CN) $_2$] $_2$.^{15,16}

In order to examine the origin of this discrepancy, we have calculated the magnetic susceptibilities for the field applied to the crystallographic a , b , and c axes (χ_a, χ_b, χ_c) and the magnetic torque amplitude for the field of 80 kOe rotated within the ab , bc , and ac plane ($\tau_{ab}^{(amp)}$, $\tau_{bc}^{(amp)}$, and $\tau_{ac}^{(amp)}$), using the one-dimensional anisotropic Heisenberg model for d electrons,

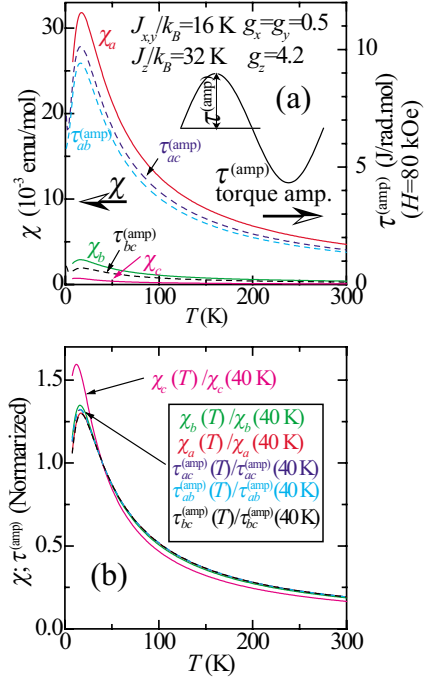


FIG. 6. (Color online) The calculations of the magnetic susceptibilities and magnetic torques. The parameters used in these calculations are $g_x=g_y=0.5$, $g_z=4.2$, $J_x=J_y=16$ K, and $J_z=32$ K. These were the same parameters used for the calculation of the magnetic properties of TPP[Fe(Pc)(CN) $_2$] $_2$. (See Ref. 12.) (a) The temperature dependence of the magnetic susceptibilities for the field applied to the crystallographic a , b , and c axes (χ_a, χ_b, χ_c) and the magnetic torque amplitude for the field rotated within the ab , bc , and ac plane [$\tau_{ab}^{(amp)}$, $\tau_{bc}^{(amp)}$, and $\tau_{ac}^{(amp)}$]. (b) Temperature dependence of these values normalized by the values at 40 K.

$$H = \mu_B \sum_i (g_{xx} H_x S_i^x + g_{yy} H_y S_i^y + g_{zz} H_z S_i^z) + \sum_i (J_x S_i^x S_{i+1}^x + J_y S_i^y S_{i+1}^y + J_z S_i^z S_{i+1}^z). \quad (3)$$

Here, the indices x , y , and z are rectangular coordinates, indicating the principal axes of the g tensor of the [Fe(Pc)(CN) $_2$] unit. (See the definition shown in Fig. 1.) The parameter $g_{\alpha\alpha}$, J_α ($\alpha=x, y, z$) are the principle values of g tensor and exchange interaction and S_i^α is the α component of the spin operator at the i th site. The parameters used in this calculations are $g_x=g_y=0.5$, $g_z=4.2$, $J_x=J_y=16$ K, and $J_z=32$ K. Details on the calculation method are described elsewhere.¹²

Figure 6(a) shows the calculated susceptibilities and torque amplitudes. Figure 6(b) demonstrates the same ones normalized by the values at 40 K. As can be seen from Fig. 6(b), the temperature dependence of the susceptibilities and torque amplitude are almost the same except $\chi_c(T)$. Those curves exhibit a peak around $T=20$ K due to the short-range-order formation of d electrons. The torque amplitude is almost proportional to H^2 (not shown in the figure).

Since $\chi_c(T)$ is significantly smaller than $\chi_a(T)$ and $\chi_b(T)$, the magnetic susceptibility data of the polycrystalline samples (χ_{poly}) of PTMA $_{0.5}$ [Fe(Pc)(CN) $_2$] \cdot CH $_3$ CN should

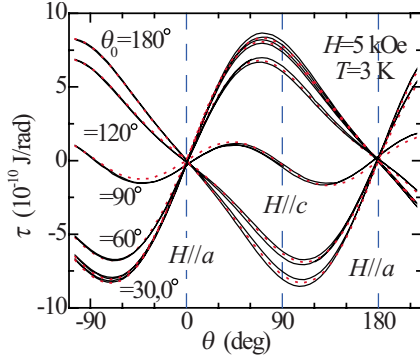


FIG. 7. (Color online) Magnetic torque curves measured at 3 K, where spontaneous magnetization exists. In this measurement, the magnetic field of 40 kOe was applied at 10 K along the direction of $\theta = \theta_0$, and the sample was cooled down to 3 K in the same field. Torque curves were measured in the reduced field of 5 kOe. Black solid lines illustrate the observed data of torque curves while the (red) dotted lines are the fit of Eq. (4) to the solid lines.

exhibit a temperature dependence similar to $\tau_{ac}^{(amp)}$. This is consistent with the observations in Fig. 5(b) above 20 K. Below 20 K, the discrepancy of χ_{poly} (obs.) from the calculations becomes obvious, while $\tau_{ac}^{(amp)}$ (obs.) is still consistent with the calculations. This can be explained if we assume that the fluctuation of the parasitic ferromagnetism, which is not considered in Eq. (3), exists below 20 K and that its influence is significant in χ_{poly} (obs.) but negligible in $\tau_{ac}^{(amp)}$ (obs.). These assumptions are plausible, since parasitic ferromagnetism below 6 K is not associated with d electrons but with π electrons, as we show later in the discussion. As we discuss in the later section, the magnetic anisotropy due to π electrons in the fluctuating-parasitic-ferromagnetism state is not so large and d electrons have a large g -tensor value. Thus, the contribution of π electrons to the torque curve, which reflects the magnetic anisotropy, should be significantly smaller than that of the d electrons.

Figure 7 shows the magnetic torque curves measured at 3 K, where spontaneous magnetization appears. In this measurement, a magnetic field of 40 kOe was applied at 10 K along the direction of $\theta = \theta_0$, and the sample was cooled down to 3 K in the same field. Then a torque curve was measured in the reduced field of 5 kOe. The black solid lines illustrate the observed data of the torque curves and the (red) dotted lines are the fits of

$$\tau(\theta) = P \sin \theta + Q \sin 2\theta \quad (4)$$

to the solid lines. In this equation, the first and second terms represent the ferromagnetic and paramagnetic contributions, respectively. As can be seen from the figure, the solid lines are well reproduced by this equation. Table I shows the parameters (P and Q) given by this fitting. It demonstrates that the paramagnetic contribution, Q , is $\sim 1.5 \times 10^{-10}$ J/rad in all the curves while the ferromagnetic contribution, P , is positive for $\theta_0 > 0$, negative for $\theta_0 < 180^\circ$, and approximately zero at $\theta_0 = 90^\circ$. These results indicate that a permanent magnetic moment due to spontaneous magnetization is

TABLE I. The parameters in the least-square fits of $\tau(\theta) = P \sin \theta + Q \sin 2\theta$ to the torque curves shown in Fig. 7.

θ_0 (deg)	$P(10^{-10}$ J/rad)	$Q(10^{-10}$ J/rad)
0	7.764	1.577
30	7.514	1.565
60	6.166	1.544
90	-0.302	1.465
120	-6.307	1.499
180	-7.769	1.526

formed along the a axis. (Note the definition of the torque sign described in the experimental section.)

Figure 8 shows the ac magnetic susceptibility data below 30 K. The increase in the real part of the susceptibility (χ_{Re}) below 5 K is probably due to the paramagnetic impurities, since it hardly exhibits frequency dependence and the imaginary part of the susceptibility (χ_{Im}) is almost zero in this temperature range. Above 13 K, frequency dependence is hardly observed in χ_{Re} , and χ_{Im} is almost zero. Below 13 K, the ac susceptibility exhibits frequency dependence. Peaks appear both in χ_{Re} and χ_{Im} . With an increase in frequency, the former peak shifts toward a higher temperature and gradually suppressed. The latter peak shifts toward a higher temperature. This result indicates that the abrupt increase in the dc magnetic susceptibility below 13 K (see Fig. 4(a)) is not a simple Curie-Weiss behavior but reflects fluctuation of spontaneous magnetization below 6 K. We will discuss this point in the later section.

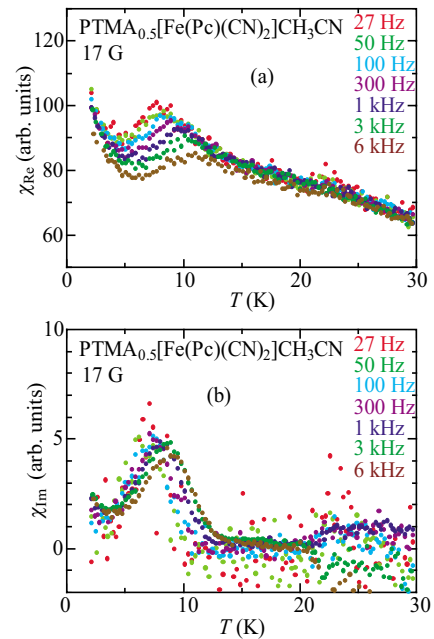


FIG. 8. (Color online) (a) The real part (χ_{Re}) and (b) the imaginary part (χ_{Im}) of the ac susceptibility of $\text{PTMA}_{0.5}[\text{Fe}(\text{Pc})(\text{CN})_2] \cdot \text{CH}_3\text{CN}$ below 30 K. Note that peaks appear in both χ_{Re} and χ_{Im} .

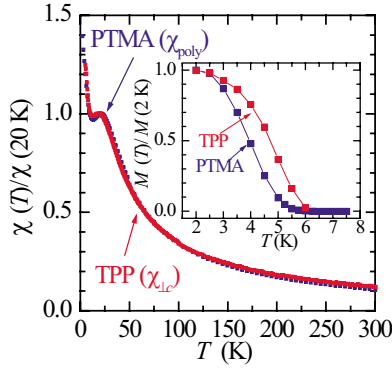


FIG. 9. (Color online) The comparison of the normalized magnetic susceptibility for $\text{PTMA}_{0.5}[\text{Fe}(\text{Pc})(\text{CN})_2] \cdot \text{CH}_3\text{CN}$ (blue) and $\text{TPP}[\text{Fe}(\text{Pc})(\text{CN})_2]_2$ (red). The former susceptibility data are for the bulk polycrystalline sample and the latter for the crystal when the field is applied perpendicular to the crystallographic c axis. The inset shows the normalized spontaneous magnetization for both salts. Note that spontaneous magnetization disappear above 6 K in both salts.

IV. DISCUSSION

The most important result obtained in this study is Fig. 7, which demonstrates the direction of spontaneous magnetization parallel to the a axis, i.e., parallel to the CN axis in $[\text{Fe}(\text{Pc})(\text{CN})_2]$ on the ac plane. Before going to the detailed discussion on this phenomenon, we compare the magnetic susceptibility of $\text{PTMA}_{0.5}[\text{Fe}(\text{Pc})(\text{CN})_2] \cdot \text{CH}_3\text{CN}$ in detail with that of $\text{TPP}[\text{Fe}(\text{Pc})(\text{CN})_2]_2$.

Figure 9 illustrates the temperature dependence of the magnetic susceptibility data for both compounds normalized by the values at $T=20$ K. The susceptibility data of $\text{PTMA}_{0.5}[\text{Fe}(\text{Pc})(\text{CN})_2] \cdot \text{CH}_3\text{CN}$ are for the bulk polycrystalline samples (χ_{poly}), and the data of $\text{TPP}[\text{Fe}(\text{Pc})(\text{CN})_2]_2$ are for a single crystal in the field applied perpendicular to the crystallographic c axis ($\chi_{\perp c}$). Note that both data exhibit similar temperature dependence. Moreover, these compounds exhibits similar spontaneous magnetization below ~ 6 K (see the inset of Fig. 9). Since both susceptibility data reflect the component for the field parallel to the CN axis (see Fig. 6 in this paper and Fig. 9 in Ref. 12), the similarity of the data indicates that *the two compounds are magnetically almost the same and their magnetic behavior is governed by the one-dimensional chain of $[\text{Fe}(\text{Pc})(\text{CN})_2]$* . On the basis of the magnetic torque measurements, we proved π electron falls into an antiferromagnetic state below 13 K in $\text{TPP}[\text{Fe}(\text{Pc})(\text{CN})_2]_2$.¹² By taking the abovementioned comparison into account, we can safely assume that π electrons in $\text{PTMA}_{0.5}[\text{Fe}(\text{Pc})(\text{CN})_2] \cdot \text{CH}_3\text{CN}$ also fall into an antiferromagnetic state below 13 K. Here we should emphasize that the direct proof of the antiferromagnetic transition of π electrons is impossible in $\text{PTMA}_{0.5}[\text{Fe}(\text{Pc})(\text{CN})_2] \cdot \text{CH}_3\text{CN}$ based on the magnetic torque measurement. Since d electrons have large g tensor, the magnetic behavior of π electrons is overwhelmed by that of d electrons, and quite difficult to investigate.¹⁷

Now we return to the discussion in Fig. 7. Since $\text{PTMA}_{0.5}[\text{Fe}(\text{Pc})(\text{CN})_2] \cdot \text{CH}_3\text{CN}$ is a d - π system, both d and

π electron can cause parasitic ferromagnetism associated with an antiferromagnetism. However, we can safely infer that the easy axis of the antiferromagnetism should be parallel to the CN axis of $[\text{Fe}(\text{Pc})(\text{CN})_2]$ in either case. Thus, the result of Fig. 7 indicates that the direction of the spontaneous magnetization is parallel to the easy axis (=CN axis) in this salt. This conclusion explicitly rules out canted ferromagnetism as the origin of the spontaneous magnetization in this salt. It also excludes the possibility that the spontaneous magnetization is a parasitic ferromagnetism associated with the antiferromagnetism of Fe(III) d electrons, since canted ferromagnetism is the only possible way for localized d electrons with $S=1/2$ spin to develop parasitic ferromagnetism.

In the case of π electrons having a delocalized character, there is another possibility. In the following, we present our model, which explains the parasitic ferromagnetism in $[\text{Fe}(\text{Pc})(\text{CN})_2]$ salts. In this model, we assume (i) antiferromagnetic exchange interaction between d spins on Fe(III), (ii) antiferromagnetic state of π electrons in Pc ring below 13 K, (iii) ferromagnetic interaction between d and π electrons on one $[\text{Fe}(\text{Pc})(\text{CN})_2]$ molecule, and (iv) charge-ordering phenomenon for the π electron system.

Assumption (i) has been already proved for $\text{PTMA}_{0.5}[\text{Fe}(\text{Pc})(\text{CN})_2] \cdot \text{CH}_3\text{CN}$ (see Fig. 6) as well as for $\text{TPP}[\text{Fe}(\text{Pc})(\text{CN})_2]_2$. The assumption (ii) was proved for $\text{TPP}[\text{Fe}(\text{Pc})(\text{CN})_2]_2$. As we have described above, it is ascertained also in $\text{PTMA}_{0.5}[\text{Fe}(\text{Pc})(\text{CN})_2] \cdot \text{CH}_3\text{CN}$. As for assumption (iii), it should be mentioned that the large spin-flop field observed in $\text{TPP}[\text{Fe}(\text{Pc})(\text{CN})_2]_2$ suggests a large d - π interaction, although the sign of the d - π interaction, whether it is ferromagnetic or antiferromagnetic, has not yet been clarified experimentally. Very recently, this interaction was suggested to be ferromagnetic on the basis of a quantum chemical calculation.⁶ As for assumption (iv), we should note that the charge-ordering phenomenon is generally approved in regular-stack molecular conductors having a quarter-filled (or three-quarter-filled) conduction band.^{18,19} This phenomenon was experimentally suggested in $\text{TPP}[\text{Co}(\text{Pc})(\text{CN})_2]_2$, which is isostructural with $\text{TPP}[\text{Fe}(\text{Pc})(\text{CN})_2]_2$ but does not have a local magnetic moment.²⁰ Since $\text{TPP}[\text{Fe}(\text{Pc})(\text{CN})_2]_2$ has a local magnetic moment associated with d electrons, the situation is not completely the same as those described above. However, a $4k_F$ diffuse streak was recently found in $\text{TPP}[\text{Fe}(\text{Pc})(\text{CN})_2]_2$ at low temperatures below 80 K.²¹ This finding provides some basis for assumption (iv).

Based on these assumptions, we propose the charge-ordered-ferrimagnetism model shown in Fig. 10(a) for the parasitic ferromagnetism in $[\text{Fe}(\text{Pc})(\text{CN})_2]$. In this model, an antiferromagnetic order of Fe(III) d spins coexists with that of π spins. Both have $4k_F$ periodicity, $2b$ in the real space for $\text{PTMA}_{0.5}[\text{Fe}(\text{Pc})(\text{CN})_2] \cdot \text{CH}_3\text{CN}$. Since π spins are also charge ordered with $4k_F$ periodicity, parasitic ferromagnetism should appear for the direction (projected in the ac plane) parallel to the a axis (easy axis).²² This is a kind of ferrimagnetic order. However the charge-rich and charge-poor sites are not fixed in this ferrimagnetic state. Thus, domain structures, for example, shown in Figs. 10(b) and 10(c), should be easily formed in a sample cooled in the zero field. In the case of Fig. 10(b), the domain boundary comes from

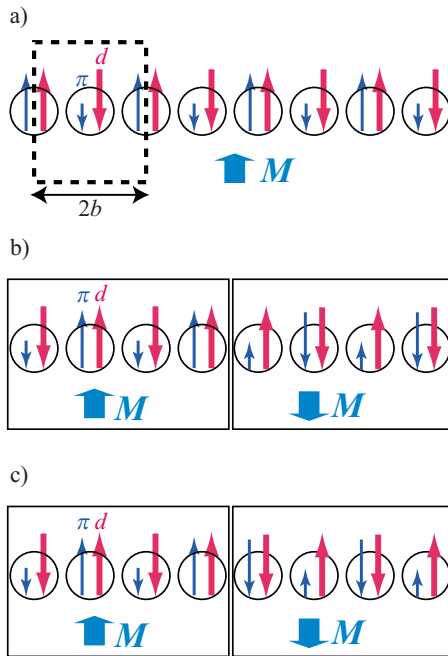


FIG. 10. (Color online) (a) The charge-ordered-ferrimagnetism model, which explains the parasitic ferromagnetism in $[\text{Fe}(\text{Pc})(\text{CN})_2]$ salts. (b) and (c) Possible domain structures in the charge-ordered-ferrimagnetism model described above. Phase inconsistency in the antiferromagnetic order of d spins (b) or in the charge order of π electrons (a) forms the domain boundary.

the phase inconsistency in the antiferromagnetic order of d electrons while it comes from the phase inconsistency in the charge order of π electrons in the case of Fig. 10(c). When a sample is cooled in a finite field, an energetically favored domain structure is selectively grown. This results in the spontaneous magnetization observed in $[\text{Fe}(\text{Pc})(\text{CN})_2]$ salts.

Domain size in this model should be temperature dependent, and not so large unless at extremely low temperature, because of the one dimensionality of the system. When the domain size becomes too small, superparamagnetic behavior should appear instead of spontaneous magnetization, and anisotropic magnetization of π electrons is considerably weakened. The latter is due to the cancellation of the effective

magnetic moment along the easy axis. [See Figs. 10(b) and 10(c).] In such a state, frequency dependence of the ac magnetic susceptibility should be detected and magnetic torque of π electrons are overwhelmed by that of d electrons. This consideration is consistent with the ac susceptibility data below 13 K (see Fig. 8) and with the torque amplitude data [see Fig. 5(b)].

At the end of this section, we discuss the possibility of the fluctuating parasitic ferromagnetism above 13 K up to 20 K. We proposed this possibility for Fig. 5(b) in Sec. III. Although the fluctuation below 13 K was proved by the ac susceptibility data up to 6 kHz, the data do not show any indication of the fluctuation above 13 K. However, we believe such fluctuation should exist even above 13 K. Since the domain size of the ferrimagnetism should be quite small above 13 K, higher frequency and more sensitive measurements are necessary in order to detect the fluctuation in the ac susceptibility measurements above 13 K.

V. CONCLUSIONS

In summary, we have demonstrated that the magnetic properties of d electrons in $\text{PTMA}_{0.5}[\text{Fe}(\text{Pc})(\text{CN})_2] \cdot \text{CH}_3\text{CN}$ salt at temperatures above 20 K is well described by the one-dimensional anisotropic Heisenberg model. We proved the spontaneous magnetization parallel to the easy axis in this salt. Based on this finding, we propose a charge-ordered-ferrimagnetism model, where parasitic ferromagnetism is formed as a result of ferromagnetic π - d interaction, the charge order of the π electrons, and the antiferromagnetic order of the d electrons. This model is commonly applicable to the conducting salts of $[\text{Fe}(\text{Pc})(\text{CN})_2]$ and their derivatives.

ACKNOWLEDGMENTS

The authors acknowledge valuable discussion with M. Takigawa at ISSP. This work was supported by a Grant-in-Aid for Scientific Research on Priority Areas of “Molecular Conductors” (Grant No. 15073207) from the Ministry of Education, Culture, Sports, Science and Technology, and a Grant-in-Aid for Scientific Research (B: Grant No. 18350070) from Japan Society for the Promotion of Science.

¹N. Hanasaki, M. Matsuda, H. Tajima, T. Naito, and T. Inabe, *J. Phys. Soc. Jpn.* **72**, 3226 (2003).

²T. Inabe and H. Tajima, *Chem. Rev. (Washington, D.C.)* **104**, 5503 (2004).

³M. Matsuda, T. Naito, T. Inabe, N. Hanasaki, and H. Tajima, *J. Mater. Chem.* **11**, 2493 (2001).

⁴M. Matsuda, T. Naito, T. Inabe, N. Hanasaki, H. Tajima, T. Otsuka, K. Awaga, B. Narymbetov, and H. Kobayashi, *J. Mater. Chem.* **10**, 631 (2000).

⁵M. Matsuda, T. Asari, T. Naito, T. Inabe, N. Hanasaki, and H. Tajima, *Bull. Chem. Soc. Jpn.* **76**, 1935 (2003).

⁶D. E. C. Yu, M. Matsuda, H. Tajima, A. Kikuchi, T. Taketsugu,

N. Hanasaki, T. Naito, and T. Inabe, *J. Mater. Chem.* **19**, 718 (2009).

⁷C. Hotta, M. Ogata, and H. Fukuyama, *Phys. Rev. Lett.* **95**, 216402 (2005).

⁸N. Hanasaki, M. Matsuda, H. Tajima, E. Ohmichi, T. Osada, T. Naito, and T. Inabe, *J. Phys. Soc. Jpn.* **75**, 033703 (2006).

⁹Y. Tokura, A. Urushibara, Y. Moritomo, R. Arima, A. Asamitsu, G. Kido, and N. Furukawa, *J. Phys. Soc. Jpn.* **63**, 3931 (1994).

¹⁰F. Goze, V. N. Laukhin, L. Brossard, A. Audouard, J. P. Ulmet, S. Askenazy, T. Naito, H. Kobayashi, A. Kobayashi, M. Tokumoto, and P. Cassoux, *Europhys. Lett.* **28**, 427 (1994).

¹¹M. Matsuda, N. Hanasaki, H. Tajima, T. Naito, and T. Inabe, *J. Phys. Chem. Solids* **65**, 749 (2004).

- ¹²H. Tajima, G. Yoshida, M. Matsuda, K. Nara, K. Kajita, Y. Nishio, N. Hanasaki, T. Naito, and T. Inabe, *Phys. Rev. B* **78**, 064424 (2008).
- ¹³E. Ohmichi and T. Osada, *Rev. Sci. Instrum.* **73**, 3022 (2002).
- ¹⁴In this paper, we define $\text{PTMA}_{0.5}[\text{FePc}(\text{CN})_2] \cdot \text{CH}_3\text{CN}$ as the unit of “mol.”
- ¹⁵N. Hanasaki, H. Tajima, M. Matsuda, T. Naito, and T. Inabe, *Phys. Rev. B* **62**, 5839 (2000).
- ¹⁶N. Hanasaki, M. Matsuda, H. Tajima, T. Naito, and T. Inabe, *Synth. Met.* **137**, 1227 (2003).
- ¹⁷We could detect the torque component of the antiferromagnetic π electrons in the case of $\text{TPP}[\text{Fe}(\text{Pc})(\text{CN})_2]_2$, since the torque amplitude associated with d electrons are considerably suppressed due to the fourfold crystal symmetry of the crystal. This technique cannot be applied to $\text{PTMA}_{0.5}[\text{Fe}(\text{Pc})(\text{CN})_2] \cdot \text{CH}_3\text{CN}$ which does not have a four-fold symmetry.
- ¹⁸For example, see, H. Seo, C. Hotta, and H. Fukuyama, *Chem. Rev.* **104**, 5005 (2004).
- ¹⁹Although the spin-Peierls transition is well known in the one-dimensional organic conductors, we could rule out this possibility since π electrons should fall into a singlet state in this transition.
- ²⁰N. Hanasaki, K. Masuda, K. Kodama, M. Matsuda, H. Tajima, J. Yamazaki, M. Takigawa, J. Yamaura, E. Ohmichi, T. Osada, T. Naito, and T. Inabe, *J. Phys. Soc. Jpn.* **75**, 104713 (2006).
- ²¹N. Hanasaki and Y. Nogami (unpublished).
- ²²Because we rotated the magnetic-field direction only in the ac plane, the information out of the ac plane was not available.